This article was downloaded by: *[Humble, Travis S.]*
On: *13 January 2011*
Access details: *Access Details: [subscription number 932366994]*
Publisher *Taylor & Francis*
Informa Ltd Registered in England and Wales Registered Number: 1072954 Registered office: Mortimer House, 37-41 Mortimer Street, London W1T 3JH, UK

Journal of Modern Optics
Publication details, including instructions for authors and subscription information:
http://www.informaworld.com/smpp/title~content=t713191304

Simultaneous teleportation of multiple single-photon degrees of freedom

Travis S. Humble[a]; Ryan S. Bennink[a]; Warren P. Grice[a]
[a] Oak Ridge National Laboratory, Oak Ridge, Tennessee 37831-6015, USA

First published on: 13 January 2011

To cite this Article Humble, Travis S. , Bennink, Ryan S. and Grice, Warren P.(2011) 'Simultaneous teleportation of multiple single-photon degrees of freedom', Journal of Modern Optics,, First published on: 13 January 2011 (iFirst)
To link to this Article: DOI: 10.1080/09500340.2010.543291
URL: http://dx.doi.org/10.1080/09500340.2010.543291

PLEASE SCROLL DOWN FOR ARTICLE

Full terms and conditions of use: http://www.informaworld.com/terms-and-conditions-of-access.pdf

This article may be used for research, teaching and private study purposes. Any substantial or systematic reproduction, re-distribution, re-selling, loan or sub-licensing, systematic supply or distribution in any form to anyone is expressly forbidden.

The publisher does not give any warranty express or implied or make any representation that the contents will be complete or accurate or up to date. The accuracy of any instructions, formulae and drug doses should be independently verified with primary sources. The publisher shall not be liable for any loss, actions, claims, proceedings, demand or costs or damages whatsoever or howsoever caused arising directly or indirectly in connection with or arising out of the use of this material.

Journal of Modern Optics
2011, 1–11, iFirst

Taylor & Francis
Taylor & Francis Group

Simultaneous teleportation of multiple single-photon degrees of freedom

Travis S. Humble*, Ryan S. Bennink and Warren P. Grice

Oak Ridge National Laboratory, Oak Ridge, Tennessee 37831-6015, USA

(*Received 9 June 2010; final version received 21 November 2010*)

We report how quantum information encoded into multiple photonic degrees of freedom may be simultaneously teleported using a single, common physical process. The application of teleportation to the complete quantum state of a photon, i.e. the spectral, spatial, and polarization component states, permits the full photonic Hilbert space to be used for encoding information while simultaneously enabling subspaces to be addressed individually, e.g. for quantum information processing. We analyze the feasibility of teleporting the full quantum state through numerical analysis of the fidelity under nominal experimental conditions and for different types of input states, e.g. single-photon states that are separable or entangled in the physical degrees of freedom.

Keywords: quantum teleportation; quantum information; quantum optics

Downloaded By: [Humble, Travis S.] At: 19:23 13 January 2011

1. Introduction

In quantum teleportation, quantum information is communicated from a sender Alice to a remote receiver Bob using the resource of distributed entanglement alongside a shared classical communication channel [1]. As a basic protocol of quantum information science, teleportation enables a variety of more complex protocols such as long-distance distribution of cryptographic keys [2,3] and teleportation-based quantum computing architectures [4,5]. Experimentally, quantum teleportation has been demonstrated using a variety of physical systems with advances in the teleportation of photonic states notable for the present discussion [6–8]. In particular, demonstrations of teleporting quantum information encoded into the state of a single photon have been largely facilitated by the readily available pair-wise entanglement sources derived from spontaneous parametric down conversion (SPDC) [9,10]. Moreover, the measurements necessary to implement teleportation can be performed using either linear [11,12] or nonlinear optics [7]. As an example, photonic quantum teleportation has been demonstrated using polarization as well as continuous-variable quadrature degrees of freedom [13,14], and implementations have been proposed that use either the transverse momentum [8,15], orbital angular momentum [16], or spectral [17,18] degrees of freedoms.

While these prior demonstrations have teleported information encoded into a single degree of freedom, the formalism of quantum teleportation indicates that the complete quantum state of a single photon may also be teleported. In addition to enabling fundamental studies of teleportation, the ability to teleport the complete quantum state would benefit the broader development of quantum information science by providing a means to utilize a greater portion of the photonic Hilbert space. For example, an increase in the size of the accessible Hilbert space would provide a corresponding increase in the symbol alphabet available for long-haul quantum key distribution schemes [19,20]. In addition, as each degree of freedom naturally partitions the full photon Hilbert space into subspaces, multiple qubits (or qudits) encoded into a single photon could be individually addressed through physically separable unitary operators. Consequently, simultaneously teleporting multiple qubits encoded into one photon suggests a resource efficient means of communicating multi-qubit entangled states, e.g. between separated nodes in a quantum computational network.

The features described above motivate the question of how multiple photonic degrees of freedom can be simultaneously teleported. We have previously addressed simultaneous teleportation of quantum information encoded into the spectral, transverse-spatial (angular), and polarization components of a single-photon quantum state in an idealized setting [21]. Independently, Ether and colleagues have proposed a similar strategy for complete teleportation of a single-photon field [22]. In the context of both reports, teleportation of the complete single-photon quantum

*Corresponding author. Email: humblets@ornl.gov

ISSN 0950–0340 print/ISSN 1362–3044 online
The work as part Travis Humble, Ryan Bennink and Warren Grice's official duties as Federal Government Contractors is published by permission of the Department of Energy under Contract Number DE-AC05-00OR22725. The US Government retains for itself, and others acting on its behalf, a paid-up, non-exclusive, and irrevocable worldwide license in said article to reproduce, prepare derivative works, distribute copies to the public, and perform publicly and display publicly, by or on behalf of the Government.
DOI: 10.1080/09500340.2010.543291
http://www.informaworld.com

Downloaded By: [Humble, Travis S.] At: 19:23 13 January 2011

state is performed by overlaying otherwise distinct protocols that have been separately developed for each individual degree of freedom. A crucial element in both proposals is the use of hyperentangled photon pair states, i.e. biphoton states simultaneously entangled in multiple degrees of freedom [23,24]. For example, hyperentangled biphoton states prepared using polarization and momentum degrees of freedom have been experimentally realized and used for demonstrating the complete discrimination of polarization-entangled Bell states [25] as well as for polarization-encoded superdense coding [26]. Hyperentangled states composed from three photonic degrees of freedom have also recently been demonstrated [27].

In addition to hyperentanglement, both proposals for total teleportation share the need for an entangled-state projective measurement that can simultaneously act on the polarization, spectral, and angular components of a biphoton state. In particular, it has been established previously that teleportation of an information carrying degree of freedom, e.g. polarization, is degraded by entanglement in the auxiliary, non-information carrying spectral and spatial degrees of freedom as these modes provide distinguishing state information [28,30,31]. Consequently, the required measurement must act simultaneously on all the entangled, information carrying degrees of freedom in order to effect the complete quantum state. The use of photon up-conversion followed by spectrally and spatially resolved polarization measurements has been suggested to perform this Bell-state-like measurement on the composite Hilbert space of two photons [21,22].

The present paper advances prior analyses of teleporting multiple photonic degrees of freedom by establishing expectations for the teleportation fidelity of a complete single-photon state using current sources of hyperentanglement. Section 2 explains how teleportation of quantum information encoded into the spectral degree of freedom can be implemented and continues by exploring the dependence of the spectral teleportation fidelity on the degree of spectral entanglement and bandwidth. Section 3 similarly considers transverse-spatial, or angular, teleportation, which is shown to exhibit a dependence on angular bandwidth and entanglement analogous to that found for spectral teleportation. Section 4 briefly reviews well-established methods for teleporting polarization states. The integration of these three disparate protocols for simultaneous teleportation of all three degrees of freedom is presented in Section 5 in the form of a conceptual experiment that combines these 'piece-wise' approaches into a single procedure. The fidelity expected of this setup for separable as well as spatio-spectral entangled input states is investigated. Concluding remarks on the probability for successful teleportation and the fidelity expected from simultaneous teleportation of multiple single-photon degrees of freedom are presented in Section 6.

2. Spectral teleportation

We first consider a protocol for teleporting the spectral probability amplitude of a single-photon state [17,18]. Spectral teleportation uses entanglement in the joint spectral amplitude of a biphoton state to mediate the transfer of a single-photon spectral state. Spectral entanglement arises naturally, for example, in the biphoton states generated by spontaneous parametric down conversion (SPDC), where conservation of energy and phase-matching constraints specify preparation of the joint spectral amplitude.

Consider a single, spectrally multimode photon described by the pure state

$$\left|\psi_1^{\text{spec}}\right\rangle = \int \alpha(\omega)|\omega_1\rangle \mathrm{d}\omega \tag{1}$$

where $\alpha(\omega)$ is the normalized spectral probability amplitude and $|\omega_1\rangle$ is the spectral eigenstate of photon 1 at frequency ω. The spectral amplitude represents the quantum information intended to be teleported to the receiving party. This information can be encoded using a family of (non-orthogonal) spectral amplitudes generated by varying the properties of $\alpha(\omega)$, including both the envelope and the phase. Photonic states of the form of Equation (1) can be prepared using either single-photon sources [32] or heralding with photon pair sources [33–35] in which the transverse-spatial and polarization degrees of freedom are prepared in single-mode states, e.g. using single-mode fiber and polarization beam-splitters. While the theory to follow applies equally well to mixed states, we defer that description to future work.

Spectral teleportation transfers the spectral amplitude $\alpha(\omega)$ of photon 1 to a remote photon 3, where the latter is initially prepared with photon 2 in the normalized state

$$\left|\varphi_{23}^{\text{spec}}\right\rangle = \int \mathrm{d}\omega \int \mathrm{d}\omega' f(\omega,\omega')\left|\omega_2, \omega_3'\right\rangle. \tag{2}$$

The joint spectral probability amplitude $f(\omega,\omega')$ determines the spectral entanglement of the photon pair [28]. The Schmidt decomposition of the joint spectral amplitude [29]

$$f(\omega,\omega') = \sum_{n=0}^{\infty} \lambda_n^{1/2} g_n(\omega) h_n(\omega') \tag{3}$$

given in terms of the Schmidt coefficients λ_n and the Schmidt modes $g_n(\omega)$ and $h_n(\omega')$, is spectrally entangled

Downloaded By: [Humble, Travis S.] At: 19:23 13 January 2011

when there exists more than one term in the summation of equation (3), i.e. when

$$f(\omega, \omega') \neq g_0(\omega)h_0(\omega'). \tag{4}$$

The spectral entanglement is conveniently quantified using the Schmidt number [29]

$$K_{\text{spec}} \equiv \sum_{n=0}^{\infty} \lambda_n \Big/ \sum_{n=0}^{\infty} \lambda_n^2 \tag{5}$$

which grows from unity as the number of nonzero Schmidt coefficients increases. Experimentally, the effects of spectral entanglement may be inferred from the reduced visibility of the Hong-Ou-Mandel dip when using independent sources [28,30,31,36], while estimates for the spectral entanglement generated by typical SPDC sources yield spectral Schmidt numbers as large as ~600 with the potential to be larger [36–39].

The mechanism for spectral teleportation is the up-conversion of photons 1 and 2 into a higher-frequency photon 4. Up-conversion entangles the spectral state of photon 3 with the spectral state of photon 4. A spectral measurement of photon 4 then projects photon 3 into a correlated spectral state. The measured frequency provides the necessary information to transform the spectral state of photon 3 into the form of Equation (1). As an example, photons 1 and 2 may be up-converted to yield photon 4 using sum-frequency generation (SFG). For SFG, the joint state of photons 3 and 4 may be expressed as

$$\left|\xi_{34}^{\text{spec}}\right\rangle = c\int \mathrm{d}\omega \int \mathrm{d}\omega' \int \mathrm{d}\omega'' \alpha(\omega) f(\omega', \omega'') \left|\omega_3'', (\omega + \omega')_4\right\rangle \tag{6}$$

where c is a normalization factor and perfect phase-matching has been assumed for simplicity. In Equation (6), entanglement between photons 3 and 4 is established through the overlap of the initial spectral amplitude $\alpha(\omega)$ and the joint spectral amplitude $f(\omega, \omega')$. As a result, a measurement of photon 4 transforms the state of photon 3. In its simplest form, this measurement is modeled by a projection onto the frequency eigenstate $|\Omega_4\rangle$. This spectral measurement then prepares photon 3 in the state

$$\left|\tilde{\psi}_3^{\text{spec}}\right\rangle = \eta_{\text{spec}} \int \mathrm{d}\omega \int \mathrm{d}\omega' \alpha(\omega) f(\Omega - \omega, \omega') \left|\omega_3'\right\rangle \tag{7}$$

where the tilde denotes this state as an intermediate result and η_{spec} is the normalization factor.

Equation (7) may be readily understood in the limit that photons 2 and 3 are perfectly entangled in frequency. In this limit, the joint spectral amplitude approaches the delta distribution

$$f(\omega, \omega') \to \delta(2\bar{\omega}_0 - \omega - \omega') \tag{8}$$

the Schmidt coefficients are identical, and the Schmidt number approaches infinity. This form of the joint spectral amplitude is well approximated by CW pumping of the SPDC process [30], where the quantity $2\bar{\omega}_0$ plays the role of the pump frequency. Although this CW-pumped source is impractical (the large uncertainty in emission time prevents the temporal overlap required for SFG), this example does illuminate how the properties of the joint spectrum affect teleportation. Inserting the approximate joint spectral amplitude of Equation (8) into Equation (7), the state of photon 3 after normalization is found to be

$$\left|\tilde{\psi}_3^{\text{spec}}\right\rangle = \int \mathrm{d}\omega\, \alpha(\omega) \left|(\omega - \Delta)_3\right\rangle. \tag{9}$$

In the present case, the spectral shift $\Delta = \Omega - 2\bar{\omega}_0$ is derived from the observed frequency Ω and knowledge of the pump frequency (which specifies the energy conservation condition but does not distinguish photons 2 and 3). This spectral shift is then used to transform the received state in Equation (9) to match the initial state in Equation (1). This spectral shift can be applied using either difference frequency generation (DFG) with a pump pulse having frequency Δ [40] or an acousto-optic frequency shifter driven at frequency Δ. Thus, as originally noted by Molotkov [17], unit spectral teleportation fidelity can be realized in the idealized case of infinite spectral entanglement and bandwidth.

The limiting case above suggests a protocol for performing spectral teleportation for the case of an arbitrary joint spectral amplitude in which the spectral state of Equation (7) is shifted by an amount Δ to obtain

$$\left|\psi_3^{\text{spec}}\right\rangle = \eta_{\text{spec}} \int \mathrm{d}\omega \int \mathrm{d}\omega' \alpha(\omega) f(\Omega - \omega, \omega' - \Delta) \left|\omega_3'\right\rangle. \tag{10}$$

The corresponding spectral teleportation fidelity, i.e. the magnitude squared overlap of Equation (10) with Equation (1), is calculated to be

$$F_{\text{spec}} = \left| \eta_{\text{spec}} \int \mathrm{d}\omega \int \mathrm{d}\omega' \alpha(\omega) f(\Omega - \omega, \omega' - \Delta) \alpha(\omega')^* \right|^2. \tag{11}$$

For the case that the spectral amplitude $\alpha(\omega)$ is sampled from a distribution of amplitudes $P(\alpha)$, then the ensemble-averaged fidelity is

$$\left\langle F_{\text{spec}} \right\rangle = \int P(\alpha) F_{\text{spec}}(\alpha) \mathrm{d}\alpha. \tag{12}$$

Equations (11) and (12) depend on Δ as well as the available spectral entanglement. The value of Δ that optimizes the spectral teleportation fidelity of a given spectral state depends on the properties of the

Downloaded By: [Humble, Travis S.] At: 19:23 13 January 2011

entangled photon pair, the relative bandwidths of the photons as well as the amount of spectral entanglement. The dependence of the fidelity on these parameters is discussed in detail elsewhere, but it should be noted that unit average fidelity is not expected in the case of finite entanglement [18]. However, a very high average fidelity, e.g. $\langle F_{\text{spec}}\rangle > 0.999$, can be obtained for realistic values of the relative bandwidths and the spectral entanglement.

As an example of spectral teleportation using finite spectral entanglement, consider the joint spectral amplitude of photons 2 and 3 to be expressed as the symmetric two-dimensional Gaussian amplitude

$$f(\omega,\omega') = N_{\text{spec}} \exp\left[-\frac{1}{2\gamma_{\text{spec}}^2}\left\{(\omega-\bar{\omega}_2)^2+(\omega'-\bar{\omega}_3)^2 -2\rho_{\text{spec}}(\omega-\bar{\omega}_2)(\omega-\bar{\omega}_3)\right\}\right] \tag{13}$$

with $\gamma_{\text{spec}}^2 = \sigma_{\text{spec}}^2(1-\rho_{\text{spec}}^2)$ expressed in terms of the marginal bandwidth of the photons σ_{spec} and the linear correlation between the photon frequencies $\rho_{\text{spec}} \in [1, -1]$, $\bar{\omega}_j$ the mean frequency of photon j, and N_{spec} the normalization factor. For this joint amplitude, the spectral Schmidt number, Equation (5), is found via the substitution $\rho_{\text{spec}} = \tanh 2\zeta$ to be [18]

$$K_{\text{spec}} = \cosh 2\zeta. \tag{14}$$

Assuming the input spectral state is Gaussian, as defined by

$$\alpha(\omega) = \left(\pi\sigma_{1,\text{spec}}^2\right)^{-1/4} \exp\left[-\frac{(\omega-\bar{\omega}_1)^2}{2\sigma_{1,\text{spec}}^2}\right] \tag{15}$$

the intermediate state, Equation (7), becomes

$$\left|\tilde{\psi}_3^{\text{spec}}\right\rangle = \eta_{\text{spec}} \int \mathrm{d}\omega\, \exp\left[-Q_{\text{spec}}(\omega-\varepsilon)^2\right]|\omega_3\rangle \tag{16}$$

where we define

$$Q_{\text{spec}} = \frac{a_{\text{spec}}^2\left(a_{\text{spec}}^2+1\right)}{2\sigma_{1,\text{spec}}^2\left(a_{\text{spec}}^2+1-\rho_{\text{spec}}^2\right)} \tag{17}$$

$\eta_{\text{spec}}^4 = 2Q_{\text{spec}}/\pi$, and $\varepsilon = \bar{\omega}_3 - \delta\rho_{\text{spec}}/(a_{\text{spec}}^2+1)$ with $a_{\text{spec}} = \sigma_{1,\text{spec}}/\sigma_{\text{spec}}$ the ratio between the bandwidths of photons 1 and 2 and $\delta = \Omega - \bar{\omega}_1 - \bar{\omega}_2$ the deviation of the measured frequency from the mean frequency of photon 4. It has been shown previously that by applying a spectral shift $\Delta = \varepsilon - \bar{\omega}_1$ to the prepared state (17), the corresponding spectral teleportation fidelity becomes [18]

$$F_{\text{spec}} = \sqrt{\frac{4a_{\text{spec}}^2(a_{\text{spec}}^2+1)(a_{\text{spec}}^2+1-\rho_{\text{spec}}^2)}{\left[(a_{\text{spec}}^2+1)^2-\rho_{\text{spec}}^2\right]^2}}\, e^{-\Gamma_{\text{spec}}} \tag{18}$$

where the contribution

$$\Gamma_{\text{spec}} = \frac{a_{\text{spec}}^2(a_{\text{spec}}^2+1)(\bar{\omega}_1+\Delta-\varepsilon)^2}{\left[(a_{\text{spec}}^2+1)^2-\rho_{\text{spec}}^2\right]\sigma_{1,\text{spec}}^2} \tag{19}$$

vanishes when the spectral shift Δ equals the root of the exponent.

A contour plot of the spectral teleportation fidelity F_{spec} with respect to a_{spec} and ρ_{spec} is shown in Figure 1 for the case $\delta = 0.1\sigma_{1,\text{spec}}$. Figure 1 is characterized by the four distinct corners of the contour plot. In the lower right-hand corner $(a_{\text{spec}}, \rho_{\text{spec}}) = (1, 0)$, there is no spectral entanglement but the input bandwidth matches the marginal bandwidth of photon 3; hence, $F_{\text{spec}} = 1$ by coincidence. In the lower left-hand corner $(0, 0)$, there is no spectral entanglement and the overlap between the input and output states vanishes as a_{spec} vanishes. The upper left-hand corner (0,1) corresponds to the case of infinite spectral entanglement and infinite marginal bandwidth, cf. Equation (8), such that $F_{\text{spec}} = 1$. The upper left-hand corner $(1, 1)$ corresponds to the case of infinite spectral entanglement and identical bandwidths for the input and output states. The fidelity in this case is not unity, however, as the high degree of spectral correlation between photons 2 and 3 plus the equal bandwidths of photons 1 and 2 yields a situation in which the preparation and measurement of the up-converted photon 4 yields some distinguishing information about the state of photon 3. This information is not absolute, but nonetheless produces a non-negligible decrease of the spectral fidelity as noted by the descending contour intervals.

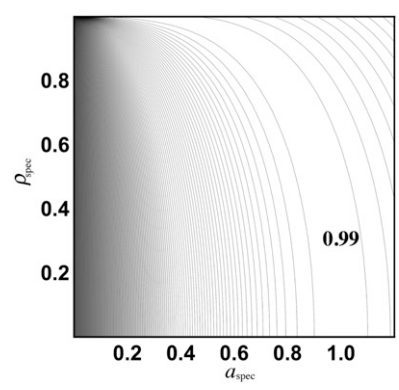

Figure 1. Contour plot of the spectral teleportation fidelity F_{spec} against the bandwidth ratio $a_{\text{spec}} = \sigma_{1,\text{spec}}/\sigma_{\text{spec}}$ and the linear correlation ρ_{spec} for the case of a Gaussian input state of unknown spectral bandwidth $\sigma_{1,\text{spec}}$ using a Gaussian joint spectral amplitude characterized by marginal spectral bandwidths σ_{spec} and linear spectral correlation ρ_{spec}. Contours begin with 0, are spaced by 0.01, and end by enclosing a region defined by $F_{\text{spec}} > 0.99$. The measured frequency is taken as $\delta = 0.1\sigma_{1,\text{spec}}$.

Downloaded By: [Humble, Travis S.] At: 19:23 13 January 2011

As an example of spectral teleportation applied to an ensemble of input states, consider a family of Gaussian spectral amplitudes $\alpha_n(\omega)$ indexed according to differences in the mean frequency $\bar{\omega}_1$. These differences in spectral amplitude manifest in the spectral fidelity via the exponent defined by Equation (19). It is apparent from Equation (19) that the exponent vanishes when $\Delta = \varepsilon - \bar{\omega}_1$. While $\bar{\omega}_1$ and ε, which depends on $\bar{\omega}_1$ via δ, are assumed unknown in this case, the dependence of the root on the explicit value of $\bar{\omega}_1$ cancels whenever $a^2_{\text{spec}} = 1 - \rho^2$. Satisfying this condition forces the exponent to vanish and yields an ensembled-average fidelity of

$$\langle F \rangle_{\bar{\omega}_1} = \sqrt{\frac{8(2-\rho^2)}{(4-\rho^2)^2}} \tag{20}$$

which approaches $\sqrt{8/9} \approx 0.94$ as $|\rho|$ approaches unity. Although this average fidelity is less than unity, it does not require any assumption about the family of spectrally shifted input states. Moreover, higher average fidelity may be obtained using other forms of spectral encoding, e.g. phase-modulated states.

Current SPDC sources of spectrally entangled photons are capable of generating spectral Schmidt numbers on the order of 600 and potentially greater [36–39]. Using Equation (14), this value of K_{spec} corresponds to a linear spectral correlation $\rho_{\text{spec}} = 0.999999$. As apparent from Figure 1, current SPDC sources of spectrally entangled biphoton states are capable of providing sufficient entanglement for demonstrating high fidelity spectral teleportation. Two such demonstrations are possible with respect to how photon 4 is measured. The first is a deterministic protocol that requires a collection of narrowband, non-overlapping detectors to span the entire frequency range populated by the up-converted photon. The second is a probabilistic protocol in which a smaller frequency range is monitored. In both cases, a non-zero bandwidth of the detector is anticipated to represent a source of noise for teleportation; however, the effect of this noise depends on the detector bandwidth relative to the spectral bandwidth of photon 4.

3. Transverse-spatial teleportation

We next consider a protocol for teleportation of the angular spectrum of a single-photon state. The transverse-momentum state of a single photon may be expressed as

$$\left|\psi_1^{\text{spat}}\right\rangle = \int u(\mathbf{q}) \left|\mathbf{q}_1\right\rangle \mathrm{d}\mathbf{q} \tag{21}$$

where $\mathbf{q}$ is the two-dimensional transverse-wave vector, $u(\mathbf{q})$ is the normalized angular spectrum (probability amplitude), and $|\mathbf{q}_1\rangle$ is the state in which photon 1 has transverse-wave vector $\mathbf{q}$. Walborn and co-workers have proposed teleportation of the angular spectrum by making use of a photon pair entangled in the transverse-spatial dimension [8]. Specifically, photons 2 and 3 are prepared in the state

$$\left|\varphi_{23}^{\text{spat}}\right\rangle = \int \mathrm{d}\mathbf{q} \int \mathrm{d}\mathbf{q}' \vartheta(\mathbf{q}, \mathbf{q}') \left|\mathbf{q}_2, \mathbf{q}'_3\right\rangle \tag{22}$$

where $\vartheta(\mathbf{q}, \mathbf{q}')$ is the joint angular spectrum (amplitude) for photon 2 to have wave vector $\mathbf{q}$ and photon 3 to have wave vector $\mathbf{q}'$. Similar to the joint spectral amplitude, the joint angular amplitude is entangled when the spatial Schmidt decomposition of $\vartheta(\mathbf{q}, \mathbf{q}')$ requires more than one term and the amount of transverse-spatial entanglement can be quantified in terms of the spatial Schmidt number K_{spat}. Experimental measures of transverse-spatial entanglement suggest that spatial Schmidt numbers on the order of 600 are obtainable by tuning the SPDC phase-matching conditions [41].

As part of the angular teleportation protocol, photons 1 and 2 are prepared in an intermediate entangled state. For example, second-harmonic generation (SHG) of photons 1 and 2 may be used to prepare

$$\left|\xi_{34}^{\text{spat}}\right\rangle = c \int \mathrm{d}\mathbf{q} \int \mathrm{d}\mathbf{q}' \int \mathrm{d}\mathbf{q}'' u(\mathbf{q}) \vartheta(\mathbf{q}', \mathbf{q}'') \left|\mathbf{q}''_3, (\mathbf{q} + \mathbf{q}')_4\right\rangle \tag{23}$$

where c is a normalization factor. The generated photon 4 is subsequently measured with respect to the transverse wave vector to invoke transformation of photon 3. In particular, Walborn and colleagues proposed a spatial measurement scheme that maps the momentum of photon 4 into a position on a plane array of point detectors using a lens of focal length f [8]. Since focusing is a unitary transformation, it does not increase or decrease the degree of spatial entanglement. The detected position vector $\boldsymbol{\rho}_D$ determines the wave vector $\mathbf{q}_D$ through the relation $\mathbf{q}_D = \boldsymbol{\kappa}\boldsymbol{\rho}_D/f$, where $\boldsymbol{\kappa}$ is the wave-vector magnitude. Following this measurement, the state of photon 3 reduces to

$$\left|\tilde{\psi}_3^{\text{spat}}\right\rangle = \eta_{\text{spat}} \int \mathrm{d}\mathbf{q} \int \mathrm{d}\mathbf{q}' u(\mathbf{q}) \vartheta\left(\mathbf{q}_D - \mathbf{q}, \mathbf{q}'\right) \left|\mathbf{q}'_3\right\rangle. \tag{24}$$

In the limit the joint spatial amplitude approaches the delta distribution, i.e. $\vartheta(\mathbf{q}, \mathbf{q}') \to \delta(2\mathbf{q}_0 - \mathbf{q} - \mathbf{q}')$, the transverse-spatial amplitude of Equation (24) is found to depend on the momentum shift $\mathbf{Q} = \mathbf{q}_D - 2\mathbf{q}_0$. In direct analogy with spectral teleportation, the momentum shift $\mathbf{Q}$ is determined from the measurement information and defines the auxiliary condition

needed to locally transform the state (24) in order to prepare the state

$$\left|\psi_3^{\text{spat}}\right\rangle = \eta_{\text{spat}} \int \mathrm{d}\mathbf{q} \int \mathrm{d}\mathbf{q}' u(\mathbf{q}) \vartheta\left(\mathbf{q}_D - \mathbf{q}, \mathbf{q}' - \mathbf{Q}\right) \left|\mathbf{q}_3'\right\rangle. \quad (25)$$

This transformation can be achieved, e.g. through difference frequency generation or a spatial light modulator [8,22].

The transverse-spatial teleportation fidelity is defined as

$$F_{\text{spat}} = \left| \eta_{\text{spat}} \int \mathrm{d}\mathbf{q} \int \mathrm{d}\mathbf{q}' u(\mathbf{q}) \vartheta\left(\mathbf{q}_D - \mathbf{q}, \mathbf{Q} - \mathbf{q}'\right) u(\mathbf{q})^* \right|^2. \quad (26)$$

Notably, this expression strongly mimics the fidelity for spectral teleportation and is expected to behave similarly with respect to entanglement, cf. spectral fidelity of Equation (11). Indeed, Walborn and colleagues have performed the numerical calculation of Equation (26) to reveal the dependence of the fidelity on the relative bandwidths of the pump and SPDC phase-matching function, i.e. the joint angular amplitude [8].

We extend that earlier analysis of transverse-spatial teleportation by Walborn and colleagues by considering a Gaussian joint angular amplitude of the form

$$\vartheta(\mathbf{q}, \mathbf{q}') = N_{\text{spat}} \exp\left[\frac{-1}{2\gamma_{\text{spat}}^2}\left\{\left(\mathbf{q} - \mathbf{q}_2\right)^2 + \left(\mathbf{q}' - \mathbf{q}_3\right)^2 - 2\rho_{\text{spat}}\left(\mathbf{q} - \mathbf{q}_2\right)\left(\mathbf{q}' - \mathbf{q}_3\right)\right\}\right], \quad (27)$$

where $\gamma_{\text{spat}}^2 = \sigma_{\text{spat}}^2(1 - \rho_{\text{spat}}^2)$ with σ_{spat} the marginal angular bandwidth of photons 2 and 3, $\rho_{\text{spat}} \in [1, -1]$ is the linear correlation between transverse momenta, and the N_{spat} is the normalization factor. Joint angular amplitudes of this form arise within the context of SPDC when both the pump and phase-matching function are approximated by Gaussian forms. Similarly, we take the normalized angular state of photon 1 as the Gaussian

$$u(\mathbf{q}) = \left(\pi\sigma_{1,\text{spat}}^2\right)^{-1/2} \exp\left[\frac{-\left(\mathbf{q} - \mathbf{q}_1\right)^2}{2\sigma_{1,\text{spat}}^2}\right]. \quad (28)$$

For this case, the intermediate angular state is expressed as

$$\left|\tilde{\psi}_3^{\text{spat}}\right\rangle = \eta_{\text{spat}} \int \mathrm{d}\mathbf{q} \exp\left[-Q_{\text{spat}}(\mathbf{q} - \boldsymbol{\varepsilon})^2\right] \left|\mathbf{q}_3\right\rangle \quad (29)$$

where

$$Q_{\text{spat}} = \frac{a_{\text{spat}}^2\left(a_{\text{spat}}^2 + 1\right)}{2\sigma_{1,\text{spat}}^2\left(a_{\text{spat}}^2 + 1 - \rho_{\text{spat}}^2\right)} \quad (30)$$

and $\boldsymbol{\varepsilon} = \mathbf{q}_3 - \mathbf{d}\rho_{\text{spat}}/(a_{\text{spat}}^2 + 1)$ with $a_{\text{spat}} = \sigma_{1,\text{spat}}/\sigma_{\text{spat}}$ the ratio between the angular bandwidth of photons 1 and 2 and $\mathbf{d} = \mathbf{q}_D - \mathbf{q}_1 - \mathbf{q}_2$ the deviation of the measured momentum with respect to the mean value of transverse momentum for photon 4. Assuming the transverse-momentum shift $\mathbf{Q} = \boldsymbol{\varepsilon} - \mathbf{q}_1$ is applied to the angular state of photon 3, the resulting analytical expression for the transverse-spatial teleportation fidelity is

$$F_{\text{spat}} = \frac{4a_{\text{spat}}^2(a_{\text{spat}}^2 + 1)(a_{\text{spat}}^2 + 1 - \rho_{\text{spat}}^2)}{\left[(a_{\text{spat}}^2 + 1)^2 - \rho_{\text{spat}}^2\right]^2} e^{-\Gamma_{\text{spat}}} \quad (31)$$

where the contribution

$$\Gamma_{\text{spat}} = \frac{a_{\text{spat}}^2(a_{\text{spat}}^2 + 1)\left|\mathbf{Q} + \mathbf{q}_3 - \mathbf{q}_1\right|^2}{\left[(a_{\text{spat}}^2 + 1)^2 - \rho_{\text{spat}}^2\right]\sigma_{1,\text{spat}}^2} \quad (32)$$

vanishes when the magnitude of momentum shift $\mathbf{Q}$ equals the root of the exponent.

A contour plot of the transverse-spatial (angular) teleportation fidelity F_{spat} with respect to a_{spat} and ρ_{spat} is shown in Figure 2 for the case $|\mathbf{Q}| = 0.1\sigma_{1,\text{spat}}$. The behavior of the transverse-spatial teleportation fidelity F_{spat} in Figure 2 is very similar to that of the spectral teleportation fidelity F_{spec} shown in Figure 1. The four corners of the plot corresponding to the four limiting behaviors of a_{spat} and ρ_{spat} can be rationalized in terms of the finite and infinite cases of bandwidth and entanglement. Note that the dependence of F_{spat} on

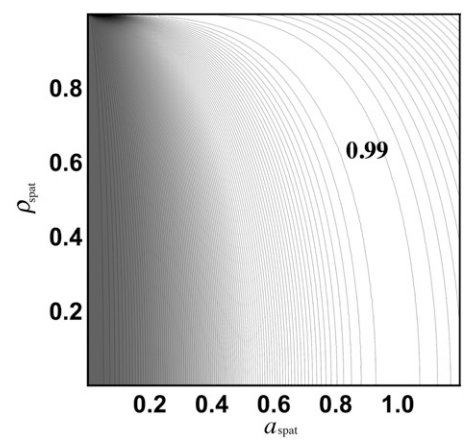

Figure 2. Contour plot of the transverse-spatial (angular) teleportation fidelity F_{spat} against the bandwidth ratio $a_{\text{spat}} = \sigma_{1,\text{spat}}/\sigma_{\text{spat}}$ and the linear correlation ρ_{spat} for the case of a Gaussian input state of unknown angular bandwidth $\sigma_{1,\text{spat}}$ using a Gaussian joint angular amplitude characterized by marginal angular bandwidth σ_{spat} and linear momentum correlation ρ_{spat}. Contours begin with 0, are spaced by 0.01, and end by enclosing a region defined by $F_{\text{spat}} > 0.99$. The measured transverse momentum is taken as $|\mathbf{d}| = 0.1\sigma_{1,\text{spat}}$.

Downloaded By: [Humble, Travis S.] At: 19:23 13 January 2011

bandwidth and entanglement is stronger than F_{spec}. This is the consequence of the two-dimensional coordinate space describing the angular probability amplitude; teleportation along either of the individual coordinate dimensions produces a dependence on these parameters similar to the spectral case, but in the two-dimensional case this dependence is squared.

4. Polarization teleportation

As noted in the Introduction, teleportation using the polarization degree of freedom is a widely referenced example of how teleportation has been achieved in practice. Several different physical mechanisms have been established for performing the requisite Bell-state measurement. Among these is the nonlinear optical implementation pioneered by Kim and colleagues that enables a complete Bell-state measurement to be performed, i.e. all four Bell polarization states can be distinguished by the measurement apparatus [7]. We will adopt this approach in Section 5, since the physical process underlying the complete polarization-encoded BSM complements the up-conversion required by the spectral and spatial protocols.

Briefly, Kim and colleagues teleport the polarization state of photon 1

$$\left|\psi_1^{\text{pol}}\right\rangle = a|h_1\rangle + b|v_1\rangle \tag{33}$$

where a and b are complex numbers specifying the amplitude for the horizontally (h) and vertically (v) polarized states, respectively. A maximally polarization-entangled state of photons 2 and 3 mediates teleportation, e.g.

$$\left|\varphi_{23}^{\text{pol}}\right\rangle = \frac{1}{\sqrt{2}}(|h_2, v_3\rangle + |v_2, h_3\rangle). \tag{34}$$

Kim and colleagues use sequential pairs of type-I and type-II SFG crystals to measure photons 1 and 2 in a polarization Bell state, cf. figure 1 of [7]. The first type-I SFG crystal transforms a pair of vertically polarized photons into a single, horizontally polarized photon, while the second type-I SFG crystal transforms a pair of horizontally polarized photons into a single, vertically polarized photon. Similarly, the first and second type-II SFG crystals transform biphoton states that are orthogonally polarized into a horizontally and vertically polarized photon, respectively. As originally noted by Kim and colleagues, the means for distinguishing between these two type-II SFG events rests on the fact that photons 1 and 2 need not have the same mean frequency. Consequently, the wavelengths of these photons can be chosen so that phase-matching requirements for the two type-II SFG events are distinct. A dichroic beam-splitter then routes the photon from the type-I and type-II crystal pairs to one of two detector stages identified by the spatial modes A and B. The biphoton polarization state prepared by these processes is

$$\begin{aligned}\left|\xi_{34}^{\text{pol}}\right\rangle = {} & (a|v_3\rangle + b|h_3\rangle)\left|h_{4,A}\right\rangle + (a|v_3\rangle - b|h_3\rangle)\left|v_{4,A}\right\rangle \\ & + (a|h_3\rangle + b|v_3\rangle)\left|h_{4,B}\right\rangle - (a|h_3\rangle - b|v_3\rangle)\left|v_{4,B}\right\rangle.\end{aligned} \tag{35}$$

Each detector stage performs a polarization resolving measurement by first erasing which-path information about the crystal that gave rise to the up-converted photon using a half-wave plate. Then, one of the four detectors denoted by the labels $\mathrm{h_A}$, $\mathrm{v_A}$, $\mathrm{h_B}$, and $\mathrm{v_B}$, signals the detection of the up-converted photon. This information alongside Equation (35) determines the unitary transformation necessary to transform the state of photon 3 to the initial qubit.

Unlike the continuous-variable spectral and transverse-spatial degrees of freedom, the discrete polarization degree of freedom carries at most a finite degree of entanglement. In particular, the polarization Schmidt number has a maximum value of $K_{\text{pol}} = 2$. The experimental effort to realize or nearly realize this finite degree of polarization entanglement can be regarded as feasible. Consequently, in the subsequent section we consider only a maximally polarization entangled state of the form presented in Equation (34).

5. Simultaneous teleportation

In Sections 2–4, component protocols for teleporting the spectral, transverse-spatial, and polarization states of a single-photon state were outlined. As each protocol destroys the photon during the measurement process, implementing teleportation across the different degrees of freedom cannot be performed sequentially. Instead, these individual protocols must be combined into a single procedure capable of simultaneously teleporting all three degrees of freedom. As all three of the described approaches depend on the up-conversion of photons 1 and 2, we propose the experimental setup shown in Figure 3 to synthesize together these implementations.

Consider the complete initial state of photon 1 to be

$$\left|\psi_1\right\rangle = \int \mathrm{d}\omega \int \mathrm{d}\mathbf{q}\left[A(\omega,\mathbf{q})\left|h(\omega,\mathbf{q})_1\right\rangle + B(\omega,\mathbf{q})\left|v(\omega,\mathbf{q})_1\right\rangle\right] \tag{36}$$

where $A(\omega,\mathbf{q})$ and $B(\omega,\mathbf{q})$ are the probability amplitudes that photon 1 has frequency ω and transverse wave vector $\mathbf{q}$ with horizontal and vertical

Downloaded By: [Humble, Travis S.] At: 19:23 13 January 2011

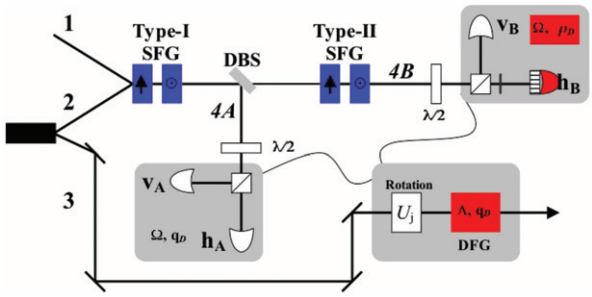

Figure 3. A conceptual experiment capable of simultaneous teleportation of the spectral, transverse-spatial, and polarization quantum states. An input photon 1 in a presumably unknown state and one member of the biphoton state generated by SPDC (black box) are mixed in a series of type-I and type-II SFG crystals for performing biphoton up-conversion in the spectral, angular, and polarization degrees of freedom to generate photon 4. A dichroic beam-splitter (DBS) distinguishes the output of the crystals by routing it to separate detector stations (gray boxes). At each detector station, the photon 4 is subjected to a frequency, momentum, and polarization resolving measurement. The measurement outcomes are the frequency Ω, the wave vector $\mathbf{q}_D$, and the polarization state, for example h_B in the figure. This measurement information is then forwarded to the post-processing stage, where transformations required to recover the initial single-photon state are applied, for example polarization rotation U_j and difference frequency generation (DFG). (The color version of this figure is included in the online version of the journal.)

polarization, respectively. The hyperentangled state for photons 2 and 3 is

$$|\varphi_{23}\rangle = \frac{1}{\sqrt{2}}\int d\omega \int d\omega' \int d\mathbf{q} \int d\mathbf{q}' P(\omega, \mathbf{q}, \omega', \mathbf{q}') \times \left[|h(\omega, \mathbf{q})_2, v(\omega', \mathbf{q}')_3\rangle + |v(\omega, \mathbf{q})_2, h(\omega', \mathbf{q}')_3\rangle\right] \tag{37}$$

where $P(\omega, \mathbf{q}, \omega', \mathbf{q}')$ is the joint probability amplitude determining the properties of the hyperentangled photon pair. Hyperentangled states of this form can be generated directly from SPDC using, for example, bulk crystals pumped by broad bandwidth pulses [23,24]. The joint amplitude P is considered to be separable with respect to physical degrees of freedom, i.e.

$$|\varphi_{23}\rangle = |\varphi_{23}^{\text{spec}}\rangle \otimes |\varphi_{23}^{\text{spat}}\rangle \otimes |\varphi_{23}^{\text{pol}}\rangle \tag{38}$$

although this need not be the case [28,31].

To invoke simultaneous teleportation in each degree of freedom, photons 1 and 2 are up-converted to generate photon 4, e.g. using spectrally and spatially phase-matched SFG. The latter process is subsequently detected by a spectrally and spatially resolving measurement apparatus. In particular, photons 1 and 2 pass through the sequence of type-I and type-II SFG crystals as shown in Figure 3, where the polarization Bell state is identified by which detector observes the photon. Assuming detection of frequency Ω, transverse-wave vector $\mathbf{q}_D$ and polarization h_B, the projected state of photon 3 is

$$|\tilde{\psi}_3\rangle = \eta \int d\omega \int d\omega' \int d\mathbf{q} \int d\mathbf{q}' P(\Omega - \omega, \mathbf{q}_D - \mathbf{q}, \omega', \mathbf{q}') \times \left[A(\omega, \mathbf{q})|H(\omega', \mathbf{q}')_3\rangle + B(\omega, \mathbf{q})|V(\omega', \mathbf{q}')_3\rangle\right] \tag{39}$$

where η is the normalization factor. Detections at the remaining measurements stations give similar results. The classical measurement information given in terms of Ω, $\mathbf{q}_D$ and h_B permits recovery of the intended quantum state. For these measurement outcomes, the identity operator is the local unitary transformation for the polarization component, while Δ and $\mathbf{Q}$ are the shifts applied to the spectral and spatial modes, respectively. These operations transform the state (39) of photon 3 to

$$|\psi_3\rangle = \eta \int d\omega \int d\omega' \int d\mathbf{q} \int d\mathbf{q}' P(\Omega - \omega, \mathbf{q}_D - \mathbf{q}, \omega' - \Delta, \mathbf{q}' - \mathbf{Q}) \times \left[A(\omega, \mathbf{q})|H(\omega', \mathbf{q}')_3\rangle + B(\omega, \mathbf{q})|V(\omega', \mathbf{q}')_3\rangle\right]. \tag{40}$$

The total teleportation fidelity of this state with respect to Equation (36) is then given by

$$F = |\eta|^2 \left| \int d\omega \int d\omega' \int d\mathbf{q} \int d\mathbf{q}' P(\Omega - \omega, \mathbf{q}_D - \mathbf{q}, \omega' - \Delta, \mathbf{q} - \mathbf{Q}) \times [A(\omega, \mathbf{q})^* A(\omega', \mathbf{q}') + B(\omega, \mathbf{q})^* B(\omega', \mathbf{q}')] \right|^2. \tag{41}$$

5.1. Separable single-photon states

When the single-photon state factorizes into spectral, spatial, and polarization components, e.g. when

$$A(\omega, \mathbf{q}) = a\, \alpha(\omega) u(\mathbf{q}) \tag{42}$$

etc., then the teleportation fidelity (41) becomes the product of the individual fidelities, i.e.

$$F = F_{\text{spec}} F_{\text{spat}} F_{\text{pol}}. \tag{43}$$

In the separable case of Equation (43), the fidelity and the entanglement in each degree of freedom must be high for reliable teleportation of the total state. However, if only a single state component is relevant, e.g. the polarization state, then poor fidelity in the spectral and transverse-spatial modes does not effect the polarization-teleportation fidelity. For example, when the joint spectral and spatial amplitudes each represent bivariate Gaussian distributions, the fidelity,

Downloaded By: [Humble, Travis S.] At: 19:23 13 January 2011

Downloaded By: [Humble, Travis S.] At: 19:23 13 January 2011

Equation (41), is the product of the individual spectral and spatial fidelities given in Equations (18) and (31), respectively, with the polarization fidelity F_{pol} assumed unity.

5.2. Non-separable single-photon states

When the single-photon state is not separable with respect to the spectral, spatial and polarization degrees of freedom, then a more general expression for the composite fidelity arises. Specifically, consider the case that the single-photon spatio-spectral amplitudes do not factorize but are represented by a spatio-spectral superposition, e.g.

$$A(\omega, \mathbf{q}) = a \sum_{n}^{N} c_n \alpha_n(\omega) u_n(\mathbf{q}) \tag{44}$$

where the coefficient c_n weights the contribution of the nth spectral amplitude $\alpha_n(\omega)$ and the nth transverse-momentum amplitude $u_n(\mathbf{q})$. For the case where these states comprise a biorthogonal basis, Equation (44) would represent a Schmidt decomposition of the spatio-spectral amplitude for photon 1; however, this condition does not hold in general. Neglecting $B(\omega, \mathbf{q})$ and the polarization state for simplicity, the composite fidelity for the spatio-spectral entangled input state is cast as

$$F = \left| \sum_{m,n} c_m^* c_n G_{\mathrm{spec}}^{m,n} G_{\mathrm{spat}}^{m,n} \right|^2 \tag{45}$$

in which

$$G_{\mathrm{spec}}^{m,n} = \int \mathrm{d}\omega \int \mathrm{d}\omega' \alpha_m^*(\omega) f(\Omega - \omega, \omega' - \Delta) \alpha_n(\omega') \tag{46}$$

and

$$G_{\mathrm{spat}}^{m,n} = \int \mathrm{d}\mathbf{q} \int \mathrm{d}\mathbf{q}' u_m^*(\mathbf{q}) \vartheta(\mathbf{q}_D - \mathbf{q}, \mathbf{q}' - \mathbf{Q}) u_n(\mathbf{q}') \tag{47}$$

represent complex-valued overlaps between the mth initial component and the nth teleported component for the spectral and spatial states, respectively. In the limit of infinite spectral and spatial entanglement and broad bandwidths, unit teleportation fidelity occurs and the quantities $G_{\mathrm{spec}}^{m,n}$ and $G_{\mathrm{spat}}^{m,n}$ represent overlaps between the non-orthogonal basis elements of the state (44). More important, it is these quantities and not the individual fidelities of isolated components that determine the composite fidelity of the state. This has the expected consequence that teleportation of the spatial and spectral components must occur simultaneously.

As an example of the spatio-spectral teleportation fidelity in Equation (45), we present the teleportation fidelity of an input state composed from the superposition of two equally weighted Gaussian amplitudes, each having the form $\alpha(\omega)\, u(\mathbf{q})$. The component amplitudes differ in the value of the bandwidths $\sigma_{1,\mathrm{spec}}$ and $\sigma_{1,\mathrm{spat}}$, cf. Equations (15) and (28). In particular, we consider the second component of the superposition to have spectral and spatial bandwidths 10 times that of the first component but the same mean values. This yields an overlap (squared magnitude) between the two spectral states of ~0.19, while the overlap between the different spatial components is ~0.039. The product of these overlaps is ~0.0015 and measures the non-orthogonality of the spatio-spectral components. The real-valued coefficients $c_0 = c_1 = 0.677871$ represent the normalized spatio-spectral superposition state.

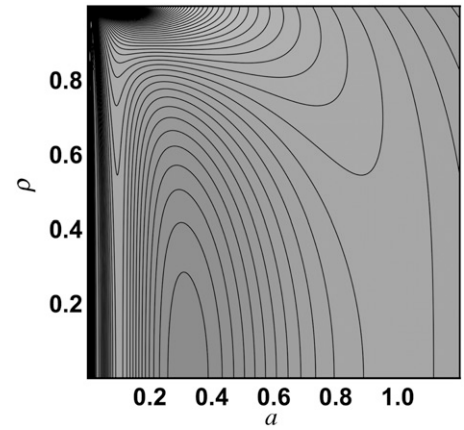

Figure 4. Contour plot of the composite teleportation fidelity F with respect to the bandwidth ratio a and the linear correlation ρ for a spatio-spectral entangled input state. Contours begin with 0, are spaced by 0.01, and increment toward the upper left-hand corner, cf. Figure 5. The measured frequency and transverse momentum of photon is taken as $\delta = 0$ and $|\mathbf{d}| = 0$.

Figure 4 presents the composite teleportation fidelity for the spatio-spectral superposition state as a function of the bandwidth ratio $a = a_{\mathrm{spec}} = a_{\mathrm{spat}}$ and the linear correlation $\rho = \rho_{\mathrm{spec}} = \rho_{\mathrm{spat}}$. The bandwidths and linear correlations (entanglement) in the spectral and spatial degrees of freedom are taken as identical for the sake of simplicity. Apparent from Figure 4 are local saddle points in the composite fidelity at $\rho = 0$ and both $a = 1.0$ and $a = 0.1$. These points correspond to cases where the initial state of photon 3 equals one or the other components in the superposition state defining photon 1. It is only for large values of entanglement ($\rho > 0.9999$) and bandwidth ($a > 0.04$) that the composite fidelity becomes large ($F > 0.99$).

Figure 5 also presents the composite teleportation fidelity for the spatio-spectral superposition state but plots this quantify with respect to the bandwidth ratio a and the Schmidt number K; recall from Equation (14) the relationship between K and ρ.

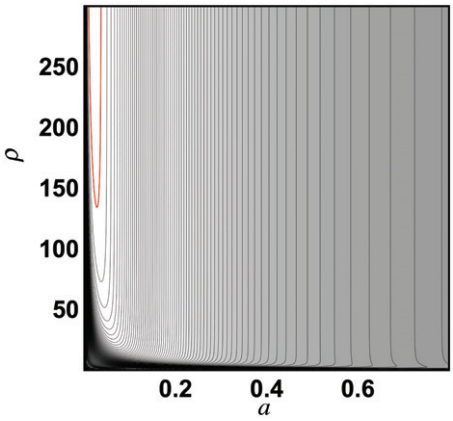

Figure 5. Contour plot of the composite teleportation fidelity F with respect to the bandwidth ratio a and the Schmidt number K for a spatio-spectral entangled input state. Contours begin with 0, are spaced by 0.01, and end with a red line denoting a fidelity of 0.99. The measured frequency and transverse momentum of photon is taken as $\delta = 0$ and $|\mathbf{d}| = 0$. (The color version of this figure is included in the online version of the journal.)

In this representation, high fidelity teleportation ($F > 0.99$) occurs for large but finite bandwidth ($a < 0.04$) and moderate Schmidt number ($K > 300$). These thresholds should be interpreted as the requirement for each degree of freedom, i.e. $K_{\text{spec}} > 300$ and $K_{\text{spat}} > 300$. As noted in Sections 2 and 3, current SPDC sources are capable of preparing biphoton states with these spatial and spectral Schmidt numbers.

6. Conclusions

We have presented a conceptual experiment for performing simultaneous teleportation of multiple photonic degrees of freedom. We have shown that the seemingly disparate protocols for teleporting single-photon spectral, angular, and polarization states may be unified through the mechanism of biphoton up-conversion. By describing a common experimental platform based on biphoton up-conversion, we have shown that these three protocols can be implemented simultaneously and, consequently, that the multiple photonic degrees of freedom characterizing a single-photon state may be simultaneously teleported.

We have also analyzed the fidelities for the individual protocols. We have shown that the composite teleportation fidelity is equivalent to the product of the individual fidelities when the single and joint probability amplitudes are separable with respect to the physical degrees of freedom. We have further shown that when the single-photon amplitude is a superposition of spatial and spectral states, i.e. spatio-spectral entangled, a high composite fidelity requires strong entanglement in both degrees of freedom.

The presented approach to simultaneous teleportation of the spectral, transverse-spatial (angular), and polarization degrees of freedom relies on biphoton up-conversion. Due to the inherently small field strength of the two photons and the small optical nonlinearities that typically mediate this process, the conversion efficiency for the platform presented is calculated to be rather low. An alternative approach would be stimulated biphoton up-conversion, e.g. a four-wave mixing process in which up conversion of the biphoton state is mediated by a strong coherent pulse and a $\chi^{(3)}$ optical medium. This can be viewed as an extension of current methods for up-converting single-photon states that use a strong pump pulse to stimulate the up conversion process in $\chi^{(2)}$ media [40,42]. The planned analysis of this approach is anticipated to yield similar, although slightly more complex, results for the teleported states.

Finally, the ability to simultaneous teleport multiple photonic degrees of freedom has the potential to greatly expand the size of the Hilbert space accessible in quantum optical implementations of quantum information protocols. Of particular interest is the ability to encode larger alphabets into these different, potentially entangled, physical modes as well as the possibility of using the different degrees of freedom to selectively address the components of a multi-qubit quantum state encoded into a single photon. Several experimental approaches have already demonstrated the utility of hyperentanglement for these types of information processing applications [19,20,24–27]. The present contribution has demonstrated the feasibility of using quantum teleportation for assisting these forms of communication and computation.

Acknowledgement

This paper has been authored by a contractor of the US Government under Contract No. DE-AC05-00OR22725. The US Government retains a non-exclusive, royalty-free license to publish or reproduce the published form of this contribution, or allow others to do so, for US Government purposes.

References

[1] Bennett, C.H.; Brassard, G.; Crépeau, C.; Josza, R.; Peres, A.; Wootters, W.K. *Phys. Rev. Lett* **1993,** *70,* 1895–1899.

[2] de Riedmatten, H.; Marcikic, I.; Tittel, W.; Zbinden, H.; Collins, D.; Gisin, N. *Phys. Rev. Lett* **2004,** *92,* 049704.

[3] Briegel, H.-J.; Dür, W.; Cirac, J.I.; Zoller, P. *Phys. Rev. Lett* **1998,** *81,* 5932–5935.

Downloaded By: [Humble, Travis S.] At: 19:23 13 January 2011

[4] Knill, E.; Laflamme, R.; Milburn, G.J. *Nature* **2001,** *409,* 46–52.
[5] Yoran, N.; Reznik, B. *Phys. Rev. Lett.* **2003,** *91,* 037903.
[6] Bouwmeester, D.; Pan, J.-W.; Mattle, K.; Eibl, M.; Weinfurter, H.; Zeilinger, A. *Nature* **1997,** *390,* 575–579.
[7] Kim, Y.-H.; Kulik, S.P.; Shih, Y. *Phys. Rev. Lett.* **2001,** *86,* 1370–1373.
[8] Walborn, S.P.; Ether, D.S.; de Matos Filho, R.L.; Zagury, N. *Phys. Rev. A* **2007,** *76,* 033801.
[9] Kwiat, P.G.; Waks, E.; White, A.G.; Appelbaum, I.; Eberhard, P.H. *Phys. Rev. A* **1999,** *60,* R773–R776.
[10] Kwiat, P.G.; Mattle, K.; Weinfurter, H.; Zeilinger, A.; Sergienko, A.V.; Shih, Y. *Phys. Rev. Lett* **1995,** *75,* 4337–4341.
[11] Braunstein, S.L.; Mann, A. *Phys. Rev. A* **1995,** *51,* R1727–R-1730.
[12] Lütkenhaus, N.; Calsmiglia, J.; Suominen, K.-A. *Phys. Rev. A* **1999,** *59,* 3295–3300.
[13] Furusawa, A.; Sørensen, J.L.; Braunstein, S.L.; Fuchs, C.A.; Kimble, H.J.; Polzik, E.S. *Science* **1998,** *282,* 706–709.
[14] Yukawa, M.; Benichi, H.; Furusawa, A. *Phys. Rev. A* **2008,** *77,* 022314.
[15] Boschi, D.; Branca, S.; De Martini, F.; Hardy, L.; Popescu, S. *Phys. Rev. Lett* **1998,** *80,* 1121–1125.
[16] Mair, A.; Vaziri, A.; Weihs, G.; Zeilinger, A. *Nature* **2001,** *412,* 313–316.
[17] Molotkov, S.N. *Phys. Lett. A* **1998,** *245,* 339–344.
[18] Humble, T.S. *Phys. Rev. A* **2010,** *81,* 062339.
[19] Ali-Kahn, I.; Broadbent, C.J.; Howell, J.C. *Phys. Rev. Lett* **2007,** *98,* 060503.
[20] Walborn, S.P.; Lemelle, D.S.; Almeida, M.P.; Souto Ribeiro, P.H. *Phys. Rev. Lett* **2006,** *96,* 090501.
[21] Humble, T.S.; Bennink, R.S.; Grice, W.P. *Proc. SPIE* **2008,** *7092,* 70920V.
[22] Ether, D.S.; Walborn, S.P.; Zagury, N. *Phys. Rev. A* **2009,** *79,* 032305.
[23] Kwiat, P.G. *J. Mod. Opt* **1997,** *44,* 2173–2184.
[24] Barreiro, J.T.; Langford, N.K.; Peters, N.A.; Kwait, P.G. *Phys. Rev. Lett.* **2005,** *95,* 260501.
[25] Barbieri, M.; Vallone, G.; Mataloni, P.; De Martini, F. *Phys. Rev. A* **2007,** *75,* 042317.
[26] Barreiro, J.T.; Wei, T.-C.; Kwiat, P.G. *Nature Phys.* **2008,** *4,* 268–269.
[27] Vallone, G.; Ceccarelli, R.; De Martini, F.; Mataloni, P. *Phys. Rev. A* **2009,** *79,* 030301(R).
[28] Humble, T.S.; Grice, W.P. *Phys. Rev. A* **2007,** *75,* 022307.
[29] Parker, S.; Bose, S.; Plenio, M.B. *Phys. Rev. A* **2000,** *61,* 032305.
[30] Grice, W.P.; Walmsley, I.A. *Phys. Rev. A* **1997,** *56,* 1627–1634.
[31] Humble, T.S.; Grice, W.P. *Phys. Rev. A* **2008,** *77,* 022312.
[32] Grangier, P.; Sanders, B.; Vuckovic, J. *New J. Phys.* [Online] **2004,** *6*. DOI: 10.1088/1367-2630/6/1/E04.
[33] U'Ren, A.B.; Silberhorn, C.; Banaszek, K.; Walmsley, I.A.; Erdmann, R.; Grice, W.P.; Raymer, M.G. *Laser Phys.* **2005,** *15,* 146–161.
[34] Mosley, P.J.; Lundeen, J.S.; Smith, B.J.; Wasylczyk, P.; U'Ren, A.B.; Silberhorn, C.; Walmsley, I.A. *Phys. Rev. Lett* **2008,** *100,* 133601.
[35] Levine, Z.H.; Fan, J.; Chen, J.; Ling, A.; Migdall, A. *Opt. Express* **2010,** *18,* 3708–3718.
[36] Avenhaus, M.; Chekhova, M.V.; Krivitsky, L.A.; Leuchs, G.; Silberhorn, C. *Phys. Rev. A* **2009,** *79,* 043836.
[37] Brida, G.; Caricato, V.; Genovese, M.; Gramegna, M.; Fedorov, M.V.; Kulik, S.P. *EPL* **2009,** *87,* 64003.
[38] Mikhailova, Yu.M.; Volkov, P.A.; Fedorov, M.V. *Phys. Rev. A* **2008,** *78,* 062327.
[39] Mauerer, W.; Silberhorn, C. *AIP Conf. Proc* **2009,** *1110,* 220–223.
[40] Takesue, H. *Phys. Rev. Lett* **2008,** *101,* 173901.
[41] Di Lorenzo Pires, H.; Monken, C.H.; van Exter, M.P. *Phys. Rev. A* **2009,** *80,* 022307.
[42] Ma, L.; Slattery, O.; Tang, X. *Opt. Express* **2009,** *17,* 14395–14404.

Downloaded By: [Humble, Travis S.] At: 19:23 13 January 2011